Editors' Suggestion | Featured in Physics

Extreme Spontaneous Deformations of Active Crystals

Xia-qing Shi,[1] Fu Cheng,[1] and Hugues Chaté[2,3]
[1]Center for Soft Condensed Matter Physics and Interdisciplinary Research, Soochow University, Suzhou 215006, China
[2]Service de Physique de l'Etat Condensé, CEA, CNRS Université Paris-Saclay, CEA-Saclay, 91191 Gif-sur-Yvette, France
[3]Computational Science Research Center, Beijing 100094, China

(Received 14 March 2023; accepted 16 June 2023; published 5 September 2023)

We demonstrate that two-dimensional crystals made of active particles can experience extremely large spontaneous deformations without melting. Using particles mostly interacting via pairwise repulsive forces, we show that such active crystals maintain long-range bond order and algebraically decaying positional order, but with an exponent η not limited by the $\frac{1}{3}$ bound given by the (equilibrium) KTHNY theory. We rationalize our findings using linear elastic theory and show the existence of two well-defined effective temperatures quantifying respectively large-scale deformations and bond-order fluctuations. The root of these phenomena lies in the sole time-persistence of the intrinsic axes of particles, and they should thus be observed in many different situations.

DOI: 10.1103/PhysRevLett.131.108301

Two-dimensional (2D) crystalline phases are usually defined by a slow algebraic decay of positional order and the presence of long-range bond order. In thermal equilibrium, the decay exponent η of the positional correlation function then increases with temperature. In many cases well described by the celebrated Kosterlitz-Thouless-Halperin-Nelson-Young (KTHNY) theory [1–5], melting of 2D crystals is a two-step process yielding an intermediate—usually hexatic—phase with short-range positional order and only quasi-long-range bond order between the crystal and liquid phases (see, e.g., [6] for a classic review). The first step is defined to be when thermally activated pairs of dislocations can unbind. This typically occurs when entropy and elastic energy for an isolated dislocation are balanced. KTHNY theory tells us that this must happen when η, which increases with temperature, reaches a value between $\frac{1}{4}$ and $\frac{1}{3}$ (for a hexagonal crystal). This bound can be seen as putting a limit on the deformability of 2D crystals.

Crystals made of active particles are maintained out of equilibrium by the persistent injection of mechanical work at local timescales and length scales, and thus are not subjected to the same constraints as their equilibrium counterparts. In particular one should not expect, on such general grounds, that KTHNY theory holds for the melting of 2D active crystals. It is then surprising that, so far, most studies of the melting of simple versions of such crystals (without chirality nor orientational order) have concluded that KTHNY theory still holds, or have assumed that it remains valid for deciding when and how melting occurs [7–18].

In this Letter, we show that 2D active crystals can experience extreme spontaneous deformations without melting: they can maintain true long-range bond order and resist unbinding of dislocation pairs even as positional order correlations decay very fast, albeit still algebraically. We argue that the decay exponent η can in fact be arbitrarily large, and rationalize our findings in terms of two well-defined effective temperatures quantifying, respectively, elastic deformations and bond-order fluctuations.

Many active crystals studied consist of spinning units or individual self-organized vortices forming a hexagonal lattice in two dimensions [19–29]. Such chiral active crystals are investigated for their specific properties such as edge modes and odd elasticity [30–33].

Active crystals with a strong alignment of the intrinsic polarities of particles have also been considered. Models demonstrated the possibility of traveling crystals [34–44] in relatively small systems. Experiments by Dauchot *et al.* investigated small crystals of polarly aligned particles [45,46]. On the theory side, the recent work of Maitra and Ramaswamy [47] makes general predictions about oriented active solids that have not been tested so far.

Here, we study the melting of simpler active crystals made of self-propelled particles subjected to pairwise repulsive forces and to rotational noise, with no or weak alignment of their polarities. Previous works have concluded or assumed that KTHNY theory remains relevant (see in particular [13–16]). They often rely on the numerical estimation of the decay of positional order correlation functions, a difficult task given that only relatively small system sizes are typically considered and that the functions usually considered are intrinsically oscillatory. Below we circumvent this problem, which allows to obtain much clearer results.

We first consider N overdamped active Brownian particles interacting via soft harmonic pairwise forces and local ferromagnetic alignment in 2D domains with periodic

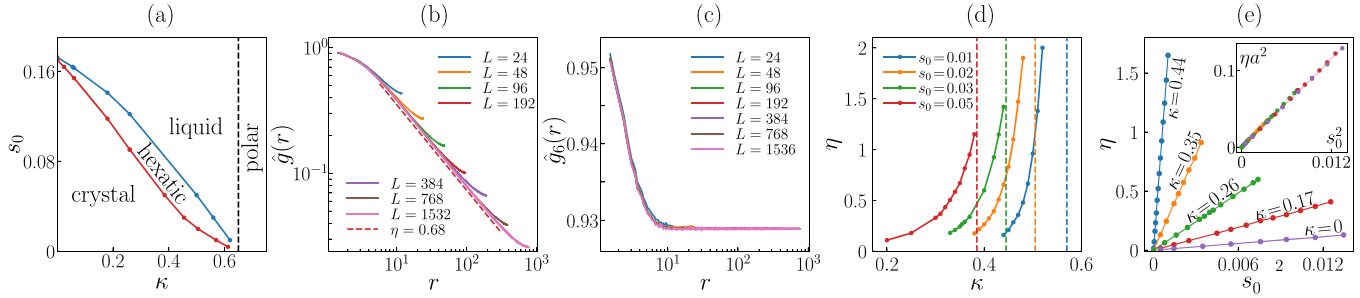

FIG. 1. Model defined by Eqs. (1) and (2) with $d_0 = D_r = 1$, $\mu_r = 1.5$. (a) Phase diagram in the (κ, s_0) plane (details about its elaboration in [48]). (b) Positional order correlation function $\hat{g}(r)$ in the crystal phase ($\kappa = 0.35$, $s_0 = 0.05$, various system sizes). (c) Same as (b) but for the bond order correlation function $\hat{g}_6(r)$. (d) Decay exponent η, extracted from plots similar to (b), as a function of κ at various s_0 values; the dashed vertical lines indicate our estimates of the melting transition. (e) Linear variation of η with s_0^2 at various κ values; inset: same data rescaled by a^2, where a was extracted from noise spectra such as in Fig. 2(a) (see main text).

boundary conditions. Their positions $\mathbf{r}_i$ and polarities θ_i obey

$$\dot{\mathbf{r}}_i = s_0 \mathbf{e}(\theta_i) + \mu_r \sum_{j\sim i} (d_0 - r_{ij}) \mathbf{e}_{ij}, \tag{1}$$

$$\dot{\theta}_i = \kappa \sum_{j\sim i} \sin(\theta_j - \theta_i) + \sqrt{2D_r}\xi_i(t), \tag{2}$$

where $\mathbf{e}(\theta_i)$ is the unit vector along θ_i, $r_{ij} = |\mathbf{r}_j - \mathbf{r}_i|$, $\mathbf{e}_{ij}$ is the unit vector pointing from j to i, the sums are taken over all j particles within distance d_0 of i, and $\xi_i(t)$ is a zero-mean Gaussian white noise with $\langle \xi_i(t)\xi_j(t')\rangle = \delta_{ij}\delta(t-t')$. Numerical details are given in [48].

We fix $d_0 = 1$, $\mu_r = 1.5$ without loss of generality, work mostly with the rotational noise strength $D_r = 1$, and vary the two remaining parameters, the self-propulsion speed s_0 and the alignment strength κ. To set the stage, we first show the phase diagram of our model in this (s_0, κ) plane [Fig. 1(a), methodological details in [48]]. Strong enough alignment ($\kappa \gtrsim 0.65$) yields global polar order ($\Psi = |\langle e^{i\theta_j}\rangle_j| > 0$). In this work, we focus on the complementary region where repulsive interactions dominate alignment, and thus $\Psi \approx 0$, with polarity correlations decaying exponentially and very fast. The crystal phase of main interest here is found at small s_0 or κ values. A liquid phase is found at large s_0 or κ values. These two phases are separated by a region of hexatic order, in line with the KTHNY two-step scenario.

Our primary interest being the stability of crystalline arrangements, we consider initially perfect hexagonal configurations with lattice step $\ell_0 = \sqrt{3}/2$ yielding a mean number density $\rho \simeq 1.54$. Below, L is the linear size in y of approximately square domains (see Ref. [48] for details).

Positional order in the crystal phase is estimated via the large-scale behavior of the two-point correlation function [49]

$$\hat{g}(r) = \left\langle \frac{\sum_{j\neq k} \delta(r - |\hat{\mathbf{r}}_j - \hat{\mathbf{r}}_k|) e^{i\hat{\mathbf{G}}\cdot[\mathbf{u}_j - \mathbf{u}_k]}}{\sum_{j\neq k} \delta(r - |\hat{\mathbf{r}}_j - \hat{\mathbf{r}}_k|)} \right\rangle_t, \tag{3}$$

where $\hat{\mathbf{r}}_i$ is the position of particle i on the initial perfect lattice, $\mathbf{u}_i(t) = \mathbf{r}_i(t) - \hat{\mathbf{r}}_i$ its displacement vector, and $\hat{\mathbf{G}}$ is one of the reciprocal vectors of the perfect lattice.

The correlation function $\hat{g}_6(r)$ of orientational bond order (which is hexatic for our triangular lattice crystals) can be defined similarly, replacing the exponential by $\psi_6^*(j)\psi_6(k)$ with the local order $\psi_6(j) = \langle e^{i6\theta_{jj'}}\rangle_{j'\sim j}$, where j' denotes the Voronoi neighbors of particle j and $\theta_{jj'}$ is the orientation of $\mathbf{r}_{j'} - \mathbf{r}_j$.

The $\hat{g}(r)$ and $\hat{g}_6(r)$ correlation functions are suited to configurations with at most bounded pairs of dislocations. They have the great advantage of not being oscillatory, so that their asymptotic behavior can be easily measured.

As expected, quasi-long-range positional order is observed in the crystal region, $\hat{g}(r) \sim r^{-\eta}$, as shown in Fig. 1(b), where results obtained at increasing system sizes are plotted [50]. Strikingly, the value $\eta \simeq 0.68$ measured in this case is much larger than $\frac{1}{3}$, the bound set by KTHNY theory, yet true long-range bond order is present [Fig. 1(c)], and no unbound dislocation (and hardly any bound dislocation pair) is found. Repeating these measurements at different values of alignment strength κ and self-propulsion force s_0, we find that η increases with both κ and s_0 [Figs. 1(d) and 1(e)] Interestingly, we observe that $\eta \propto s_0^2$ (at constant κ).

We now present general arguments advocating for the possibility to observe η values larger than $\frac{1}{3}$ in active crystals. In thermal equilibrium, linear elastic theory [4,51] leads to

$$\eta = k_B T |\hat{\mathbf{G}}|^2 \frac{3\mu + \lambda}{4\pi\mu(2\mu + \lambda)}, \tag{4}$$

where μ and λ are the Lamé elastic constants. Melting occurs roughly when entropy and elastic energy for creating a dislocation are balanced. This statement, made precise by KTHNY [6], yields the melting temperature

$$k_B T_m = \ell_0^2 \frac{\mu(\mu + \lambda)}{4\pi(2\mu + \lambda)}. \tag{5}$$

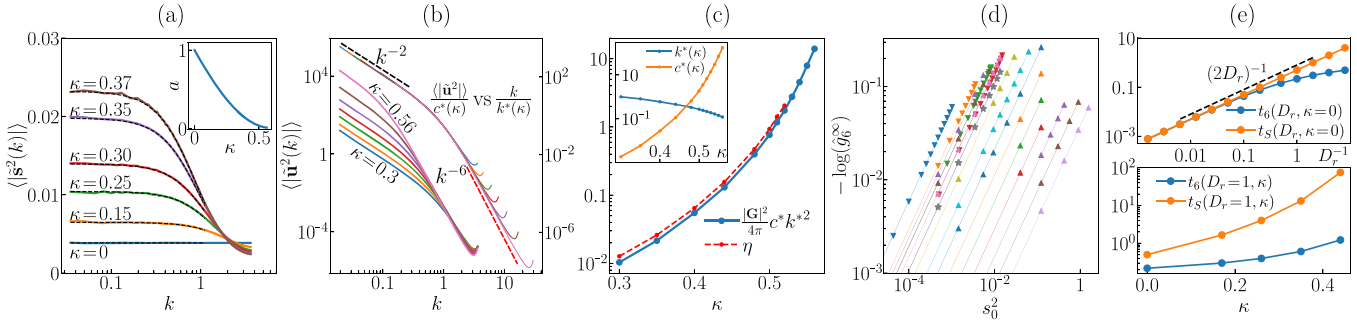

FIG. 2. (a) Spatial spectra of $\mathbf{s}$ for various κ values. Black dashed curves are fits by the function $\langle|\tilde{\mathbf{s}}^2(k)|^2\rangle = s_0^2 D_r\rho/(a+bk^2)$ obtained by solving Eq. (7) [48], from which we extract estimates of a. Inset: variation of a with κ. (b) Spatial spectra $\langle|\mathbf{u}(k)|^2\rangle$ for $\kappa = 0.3, 0.35, 0.4, 0.44, 0.48, 0.52, 0.56$ from bottom up (lower curves) and their collapse $\langle|\mathbf{u}(k)|^2\rangle/c^*(\kappa)$ vs $k/k^*(\kappa)$ obtained by choosing appropriate scaling parameters $c^*(\kappa)$ and $k^*(\kappa)$. (c) variation with κ of $|\hat{\mathbf{G}}|^2 c^* k^{*2}/4\pi$ ($|\hat{\mathbf{G}}|^2 = 4\pi^2$) and η measured as in Fig. 1 from the decay of $\hat{g}(r)$; inset: $c^*(\kappa)$ and $k^*(\kappa)$ values used to collapse spectra in (b). (d) $-\log \hat{g}_6|_{r\to\infty}$ vs s_0^2 for $D_r = 1$ and $\kappa = 0$ (gray stars), $\kappa = 0.17, 0.26, 0.35, 0.44$ (down triangles from right to left), and for various $D_r = \frac{1}{8}, \frac{1}{4}, \frac{1}{2}, 2, 5, 10, 20, 40, 80, 160, 320, 640$ at $\kappa = 0$ (up triangles) (solid lines are near perfect fits to linear functions of s_0^2) (e) variation with D_r (top) and κ (bottom) of s_0^2-rescaled temperatures t_6 and t_S extracted from fits shown in (d) and from corresponding estimates of η (see text). [$L = 384$, $s_0 = 0.05$ in (a), $s_0 = 0.01$ in (b)–(e)].

Combining these two equations by eliminating k_BT, and using $|\hat{\mathbf{G}}|^2\ell_0^2 = (16/3)\pi^2$ for triangular lattices, yields $\eta = (\mu+\lambda)(3\mu+\lambda)/3(2\mu+\lambda)^2$ at melting, an expression bounded from above by $\frac{1}{3}$.

Of course, things can be very different out of equilibrium. We argue here and show later that one can, in a sense, still invoke the two equilibrium relations (4) and (5) but at two different noise levels or effective temperatures: T_S, involved in (4), characterizes the large scale elastic deformations of the crystal structure, and T_D, involved in (5), drives dislocation motion. Given that the weak polar alignment of persistent polarities smoothes out local irregularities, one can expect $T_D < T_S$, which, when (4) and (5) are combined, yields η values at melting larger than $\frac{1}{3}$ [52].

These ideas can be made more concrete by considering the polarity field $\mathbf{s} = s_0\mathbf{e}(\theta)$. Our observation that $\eta \propto s_0^2$ suggests that $\mathbf{s}$ can be taken as an effective space- and time-correlated noise. We have calculated the spatial power spectrum of $\mathbf{s}$ [Fig. 2(a)]. The plateaus at small wave number define an effective temperature corresponding to T_S, while a lower noise level T_D can be attributed to the $k > 1$ (near lattice spacing) behavior [53]. These spectra can be superimposed by dividing them by s_0^2 (not shown), whereas the low-k plateau values corresponding to T_S increase with κ [inset of Fig. 2(a)]. Note that this is consistent with our observation that η increases with s_0^2 (linearly) and with κ [Figs. 1(d) and 1(e)].

Most of our findings can be accounted for within linear elastic theory. The equation governing the displacement field $\mathbf{u}$ can be expressed as [44,54]

$$\partial_t\mathbf{u} = (\lambda+\mu)\nabla(\nabla\cdot\mathbf{u}) + \mu\nabla^2\mathbf{u} + \mathbf{s}. \tag{6}$$

In equilibrium, $\mathbf{s}$ is a white noise defining a thermal temperature k_bT, but in our active crystal one can expect [55]

$$\partial_t\mathbf{s} = -a\mathbf{s} + b\nabla^2\mathbf{s} + \boldsymbol{\sigma} \tag{7}$$

with $\boldsymbol{\sigma}$ a white noise with $\langle\sigma_\alpha(\mathbf{r},t)\sigma_\beta(\mathbf{r}',t')\rangle = s_0^2 D_r\rho\delta_{\alpha\beta}\delta(\mathbf{r}-\mathbf{r}')\delta(t-t')$ [as can be obtained from coarse-graining Eqs. (1) and (2)]. Coefficients a and b are positive: $-a\mathbf{s}$ is a damping term accounting for the short range correlations of polarities, and the Laplacian arises from the weak aligning interactions.

The spatial spectrum of $\mathbf{u}$ can be calculated from the linear Eqs. (6) and (7) [48]. Its small wave number limit reads

$$\lim_{k\to 0}\langle|\tilde{\mathbf{u}}(k)|^2\rangle = \frac{\rho(\lambda+3\mu)}{\mu(\lambda+2\mu)}\frac{s_0^2 D_r}{2a^2k^2}, \tag{8}$$

which, compared to the equilibrium case, yields an effective temperature $T_S = \frac{1}{2}s_0^2 D_r/a^2$ [56]. Good agreement is found between linear theory and the numerical estimates of $\langle|\tilde{\mathbf{u}}(k)|^2\rangle$: at fixed s_0, varying κ, rescaling wave numbers by $k^*(\kappa)$ and spectra by a coefficient $c^*(\kappa)$ yields an excellent collapse which reveals a $1/k^2$ behavior at low k followed by a $1/k^6$ decay at high k [Fig. 2(b), and calculation in [48]]. The product $c^*(\kappa)k^{*2}(\kappa)$ provides an estimate of the prefactor of $1/k^2$ in Eq. (8), and thus, using Eq. (4), of the decay exponent η, which can be reexpressed as $\eta = (1/4\pi)|\hat{\mathbf{G}}|^2 c^* k^{*2}$. As expected, these estimates of η match very well those obtained by directly calculating the decay of $\hat{g}(r)$ [Fig. 2(c)].

Remarkably, the spectra-based η values extend even further than the direct ones, reaching $\eta \simeq 20$ for the case presented in Fig. 2(c). The direct evaluation of η breaks

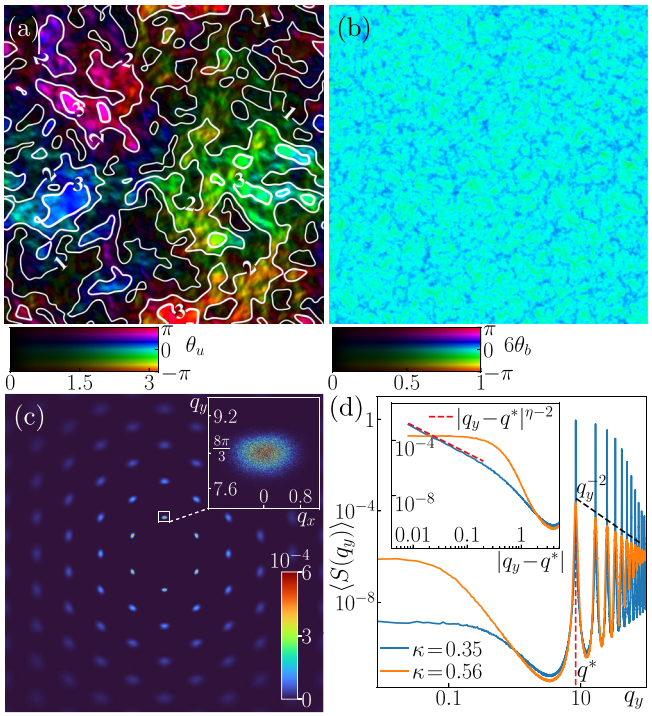

FIG. 3. Highly distorted configuration in the crystal phase for which the effective decay exponent $\eta \simeq 14$ ($\kappa = 0.56$, $s_0 = 0.01$, $L = 1536$). (a) Displacement field $\mathbf{u}$ (color is orientation, brightness is magnitude) with superimposed contour lines drawn for integer values of $|\mathbf{u}|$ in units of lattice spacing. (b) Hexatic bond order field ψ_6 [color scheme as in (a)]. (c) Instantaneous static structure factor $S(\mathbf{q}) = \rho^*(\mathbf{q})\rho(\mathbf{q})$ where $\rho(\mathbf{q}) = \langle e^{i\mathbf{q}\cdot\mathbf{r}_j}\rangle_j$ (color in linear scale); the inset is a zoom on the region of the first quasi-Bragg peak. (d) Time-averaged static structure factor $\langle S(q_y)\rangle_t$ measured at $q_x = 0$ superimposed on that obtained for $\kappa = 0.35$ for which $\eta \simeq 0.027$. Inset: zoom on the first peak located at $q = q^*$ showing an algebraic divergence $|q_y - q^*|^{\eta-2}$ only for $\kappa = 0.35$.

down when $\eta \to 2$ since then the very notion of Bragg peak with power-law divergence disappears [51]. Nevertheless, even though distortions of the crystal exceed the lattice spacing, the deformation field $\mathbf{u}$ behaves smoothly, locally preserving the crystalline order while hexatic bond order is clearly long range [Figs. 3(a) and 3(b)]. As expected, the structure factor presents a sixfold symmetry in Fourier space (testifying of crystal order), but it consists of smooth, nondiverging, noisy extended peaks [Fig. 3(c)]. The central region flattens as $|\mathbf{q}| \to 0$ and the further peaks in the high q region show a q^{-2} scaling. All this is qualitatively different from the behavior at smaller κ values where η is smaller than 2 and peaks with a power-law divergence $|q_y - q^*|^{\eta-2}$ are observed [Fig. 3(d)]. Thus, estimates of η obtained via $\langle|\tilde{\mathbf{u}}(k)|^2\rangle$ remain well defined. Contrary to direct measurements, they can be extended almost up to the crystal-hexatic transition.

We now consider the bond order properties of our active crystals. At fixed parameter values, one can estimate the asymptotic nonzero value $\hat{g}_6^\infty = \lim_{L,r\to\infty}\hat{g}_6(r)$ from data

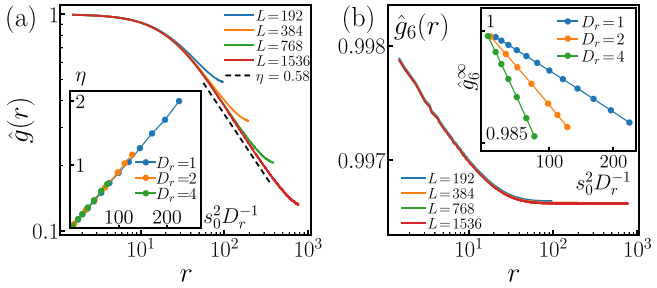

FIG. 4. Crystal phase of active Brownian particles interacting via a repulsive WCA potential (initial conditions as in other figures, $\rho\sigma^2 = 1.25$, $\epsilon = \mu_r = 1$). (a) $\hat{g}(r)$ in the crystal phase ($s_0 = 8$, various system sizes), showing a decay exponent $\eta \simeq 0.58$; inset: η vs s_0^2/D_r for various D_r and s_0 values ($L = 768$). (b) Same as (a) but for the bond order correlation function $\hat{g}_6(r)$; inset: $\hat{g}_6^\infty$ vs s_0^2/D_r.

such as those in Fig. 1(c). In equilibrium, linear theory predicts that $\hat{g}_6^\infty$ decreases exponentially with temperature [51]. Here we do observe that $-\log(\hat{g}_6^\infty) \sim s_0^2$ for a variety of D_r and κ values [Fig. 2(d)]. This suggests the existence of a "bond-order temperature" $T_6 = t_6(D_r,\kappa)s_0^2$ with the rescaled temperature $t_6(D_r,\kappa)$ proportional to the prefactor of s_0^2 for the lines of Fig. 2(d). To be a meaningful temperature, though, the absolute value of T_6 must be adjusted so that it coincides with T_S in the equilibrium $D_r \to \infty$ limit where the system is subjected to a white noise. Since $T_S = (D_r/2a^2)s_0^2$, we define a rescaled temperature $t_S(D_r,\kappa) = T_S/s_0^2 = D_r/2a^2$, and globally adjust t_6 so that it coincides with t_S in the $D_r \to \infty$ limit. Our data then show how t_6 departs from t_S as D_r decreases, even in the absence of alignment ($\kappa = 0$). Similarly, $t_6 < t_S$, and increasingly so, when κ is increased [Fig. 2(e)]. That T_6 can easily be much smaller than T_S indicates that fluctuations of bond order can remain rather gentle while positional order ones are strong. Since bond disorder helps trigger the unbinding of dislocation pairs, one can argue that T_6 is closely related to T_D, confirming the scenario introduced earlier.

We finally show that our results are not specific to soft interaction potentials and confirm—this was already shown in Fig. 2(e)—that alignment is not necessary to observe extremely deformable active crystals. We revisited the crystals of active Brownian particles investigated recently by Paliwal and Dijkstra [16], which were declared to exhibit a "defectless hexatic phase," a conclusion drawn from positional order correlations decaying faster than a $\eta = \frac{1}{3}$ power law. Particles now interact via only pairwise, hardcore repulsive forces. Angles follow Eq. (2) with $\kappa = 0$ and positions are governed by

$$\dot{\mathbf{r}}_i = s_0\mathbf{e}(\theta_i) + \mu_r\sum_{j\sim i}\partial_r U(r_{ij})\mathbf{e}_{ij}, \tag{9}$$

where $U(r) = 4\varepsilon[(\sigma/r)^{12} - (\sigma/r)^6] + \varepsilon$ is a repulsive Weeks-Chandler-Andersen potential cutoff at $r_c = 2^{1/6}\sigma$.

Using parameter values similar to those at which "defect-less hexatic order" was reported but considering larger systems, we find instead a bona fide crystal phase, with clear algebraic decay of positional order—and η values easily larger than $\frac{1}{3}$—, while bond orientational order is truly long range (Fig. 4) [58]. Varying D_r and s_0 we find again that η depends only on $T_S = s_0^2/2D_r$, while $\hat{g}_6^\infty$ does not (insets of Fig. 4), indicating that, in this case also, $T_6 < T_S$.

To summarize, we have shown that fluctuations in 2D active crystals can induce extremely large deformations without melting: bond order remains long range, and positional order decays algebraically, but with an exponent η not limited by the $\frac{1}{3}$ bound given by KTHNY theory. For the simple cases studied, linear elastic theory allowed us to rationalize our findings in terms of well-defined effective temperatures T_S and T_6 quantifying, respectively, large-scale deformations and bond-order fluctuations. We found in particular that T_6, which is expected to control melting, can be much smaller than T_S, allowing thus extreme spontaneous deformations while long-range bond order is preserved. The root of our results, obtained both with and without weak alignment of the intrinsic axes of active particles, lies in the sole time persistence of these polarities [59]. We thus expect similar phenomena to be present in other types of active crystals, such as those made of chiral or spinning units. Generalizing further, the key ingredient can be seen to be the existence of some effective time-correlated local noise. In line with this idea, preliminary results indicate that even passive crystals submitted to an active bath can display large spontaneous deformations.

We thank Benoît Mahault for a careful reading of the manuscript. This work is supported by the National Natural Science Foundation of China (Grants No. 12275188 and No. 11922506).

[1] J. M. Kosterlitz and D. J. Thouless, J. Phys. C **5**, L124 (1972).
[2] J. M. Kosterlitz and D. J. Thouless, J. Phys. C **6**, 1181 (1973).
[3] B. I. Halperin and D. R. Nelson, Phys. Rev. Lett. **41**, 121 (1978).
[4] D. R. Nelson and B. I. Halperin, Phys. Rev. B **19**, 2457 (1979).
[5] A. P. Young, Phys. Rev. B **19**, 1855 (1979).
[6] K. J. Strandburg, Rev. Mod. Phys. **60**, 161 (1988).
[7] J. Bialké, T. Speck, and H. Löwen, Phys. Rev. Lett. **108**, 168301 (2012).
[8] G. S. Redner, M. F. Hagan, and A. Baskaran, Phys. Rev. Lett. **110**, 055701 (2013).
[9] R. Singh and R. Adhikari, Phys. Rev. Lett. **117**, 228002 (2016).
[10] S. Thutupalli, D. Geyer, R. Singh, R. Adhikari, and H. A. Stone, Proc. Natl. Acad. Sci. U.S.A. **115**, 5403 (2018).
[11] L. F. Cugliandolo, P. Digregorio, G. Gonnella, and A. Suma, Phys. Rev. Lett. **119**, 268002 (2017).
[12] P. Digregorio, D. Levis, A. Suma, L. F. Cugliandolo, G. Gonnella, and I. Pagonabarraga, Phys. Rev. Lett. **121**, 098003 (2018).
[13] P. Digregorio, D. Levis, A. Suma, L. F. Cugliandolo, G. Gonnella, and I. Pagonabarraga, J. Phys. Conf. Ser. **1163**, 012073 (2019).
[14] J. U. Klamser, S. C. Kapfer, and W. Krauth, Nat. Commun. **9**, 5045 (2018).
[15] A. Pasupalak, L. Yan-Wei, R. Ni, and M. Pica Ciamarra, Soft Matter **16**, 3914 (2020).
[16] S. Paliwal and M. Dijkstra, Phys. Rev. Res. **2**, 012013(R) (2020).
[17] B. Loewe, M. Chiang, D. Marenduzzo, and M. C. Marchetti, Phys. Rev. Lett. **125**, 038003 (2020).
[18] P. Digregorio, D. Levis, L. F. Cugliandolo, G. Gonnella, and I. Pagonabarraga, Soft Matter **18**, 566 (2022).
[19] I. H. Riedel, K. Kruse, and J. Howard, Science **309**, 300 (2005).
[20] Y. Sumino, K. H. Nagai, Y. Shitaka, D. Tanaka, K. Yoshikawa, H. Chaté, and K. Oiwa, Nature (London) **483**, 448 (2012).
[21] N. H. P. Nguyen, D. Klotsa, M. Engel, and S. C. Glotzer, Phys. Rev. Lett. **112**, 075701 (2014).
[22] K. Yeo, E. Lushi, and P. M. Vlahovska, Phys. Rev. Lett. **114**, 188301 (2015).
[23] Y. Goto and H. Tanaka, Nat. Commun. **6**, 5994 (2015).
[24] A. P. Petroff, X.-L. Wu, and A. Libchaber, Phys. Rev. Lett. **114**, 158102 (2015).
[25] N. Oppenheimer, D. B. Stein, and M. J. Shelley, Phys. Rev. Lett. **123**, 148101 (2019).
[26] Z.-F. Huang, A. M. Menzel, and H. Löwen, Phys. Rev. Lett. **125**, 218002 (2020).
[27] M. James, D. A. Suchla, J. Dunkel, and M. Wilczek, Nat. Commun. **12**, 5630 (2021).
[28] T. H. Tan, A. Mietke, J. Li, Y. Chen, H. Higinbotham, P. J. Foster, S. Gokhale, J. Dunkel, and N. Fakhri, Nature (London) **607**, 287 (2022).
[29] N. Oppenheimer, D. B. Stein, M. Y. B. Zion, and M. J. Shelley, Nat. Commun. **13**, 804 (2022).
[30] B. C. van Zuiden, J. Paulose, W. T. M. Irvine, D. Bartolo, and V. Vitelli, Proc. Natl. Acad. Sci. U.S.A. **113**, 12919 (2016).
[31] C. Scheibner, A. Souslov, D. Banerjee, P. Surówka, W. T. M. Irvine, and V. Vitelli, Nat. Phys. **16**, 475 (2020).
[32] E. S. Bililign, F. Balboa Usabiaga, Y. A. Ganan, A. Poncet, V. Soni, S. Magkiriadou, M. J. Shelley, D. Bartolo, and W. T. M. Irvine, Nat. Phys. **18**, 212 (2022).
[33] L. Braverman, C. Scheibner, B. VanSaders, and V. Vitelli, Phys. Rev. Lett. **127**, 268001 (2021).
[34] G. Grégoire, H. Chaté, and Y. Tu, Physica (Amsterdam) **181D**, 157 (2003).
[35] E. Ferrante, A. E. Turgut, M. Dorigo, and C. Huepe, Phys. Rev. Lett. **111**, 268302 (2013).
[36] E. Ferrante, A. Emre Turgut, M. Dorigo, and C. Huepe, New J. Phys. **15**, 095011 (2013).
[37] A. M. Menzel, J. Phys. Condens. Matter **25**, 505103 (2013).
[38] A. M. Menzel and H. Löwen, Phys. Rev. Lett. **110**, 055702 (2013).

[39] A. M. Menzel, T. Ohta, and H. Löwen, Phys. Rev. E **89**, 022301 (2014).
[40] L. Ophaus, S. V. Gurevich, and U. Thiele, Phys. Rev. E **98**, 022608 (2018).
[41] F. Alaimo, S. Praetorius, and A. Voigt, New J. Phys. **18**, 083008 (2016).
[42] C. A. Weber, C. Bock, and E. Frey, Phys. Rev. Lett. **112**, 168301 (2014).
[43] S. Rana, M. Samsuzzaman, and A. Saha, Soft Matter **15**, 8865 (2019).
[44] C. Huang, L. Chen, and X. Xing, Phys. Rev. E **104**, 064605 (2021).
[45] G. Briand, M. Schindler, and O. Dauchot, Phys. Rev. Lett. **120**, 208001 (2018).
[46] M. N. van der Linden, L. C. Alexander, D. G. A. L. Aarts, and O. Dauchot, Phys. Rev. Lett. **123**, 098001 (2019).
[47] A. Maitra and S. Ramaswamy, Phys. Rev. Lett. **123**, 238001 (2019).
[48] See Supplemental Material at http://link.aps.org/supplemental/10.1103/PhysRevLett.131.108301 for numerical details of particle simulations, phase diagram, comparison with other correlations functions, and some results of linearised theories.
[49] M. Engel, J. A. Anderson, S. C. Glotzer, M. Isobe, E. P. Bernard, and W. Krauth, Phys. Rev. E **87**, 042134 (2013).
[50] Measurements performed using the more traditional, but oscillatory correlation function $g(r) = \langle \sum_{j\neq k} \delta(r - |\mathbf{r}_j - \mathbf{r}_k|) e^{i\mathbf{G}\cdot[\mathbf{r}_j - \mathbf{r}_k]} / \sum_{j\neq k} \delta(r - |\mathbf{r}_j - \mathbf{r}_k|) \rangle_t$, shown in [48], give essentially the same results, albeit with not as clean an algebraic decay as observed with $\hat{g}(r)$.
[51] M. Kardar, *Statistical Physics of Fields* (Cambridge University Press, Cambridge, England, 2007).
[52] Note that μ and λ in principle depend on temperature, something we neglect in this rough argument.
[53] For $\kappa = 0$ (no alignment), unsurprisingly, the spatial spectrum is flat. This does not necessarily mean that $T_S = T_D$, since the **s** field is still time correlated.
[54] P. M. Chaikin and T. C. Lubensky, *Principles of Condensed Matter Physics* (Cambridge University Press, Cambridge, England, 1995).
[55] See, e.g., discussion of the time-dependent Ginzburg-Landau equation in Kardar's book [51].
[56] In the $\kappa = 0$ nonaligning limit, where the **s** spectrum is flat, one has $a = D_r$, and thus $T_S = \frac{1}{2} s_0^2 / D_r$, as expected for active Brownian particles; see, e.g., [57].
[57] M. E. Cates and J. Tailleur, Annu. Rev. Condens. Matter Phys. **6**, 219 (2015).
[58] Note that this is only observed beyond a crossover scale of the order of 100 lattice steps, a sizable numerical difficulty, which comes in addition to having to use small timesteps.
[59] The reader might wonder why most of our results are for the rather "exotic" case of weak alignment. The main reason is practical: one can use much larger time steps in this case than with the hardcore WCA potential, saving about 1 order of magnitude of computation time.